

# Chromatic Pupilloperimetry Measures Correlate With Visual Acuity and Visual Field Defects in Retinitis Pigmentosa Patients

Ifat Sher<sup>1,2</sup>, Yisroel Tucker<sup>1</sup>, Maya Gurevich<sup>1,2</sup>, Amit Hamburg<sup>1,2</sup>, Ettl Bubis<sup>1,2</sup>, Jonathan Kfir<sup>1,2</sup>, Shlomit Zorani<sup>1,2</sup>, Estela Derazne<sup>2</sup>, Alon Skaat<sup>1-3</sup>, and Ygal Rotenstreich<sup>1,2</sup>

<sup>1</sup> Goldschleger Eye Institute, Sheba Medical Center, Tel-Hashomer, Israel

<sup>2</sup> Sackler Faculty of Medicine, Tel Aviv University, Tel Aviv, Israel

<sup>3</sup> The Sam Rothberg Glaucoma Center, Goldschleger Eye Institute, Sheba Medical Center, Tel-Hashomer, Israel

**Correspondence:** Ygal Rotenstreich, Goldschleger Eye Institute, Sheba Medical Center, Tel Hashomer 52621, Israel. e-mail: [ygal.rotenstreich@sheba.health.gov.il](mailto:ygal.rotenstreich@sheba.health.gov.il)

**Received:** January 22, 2020

**Accepted:** April 20, 2020

**Published:** July 8, 2020

**Keywords:** retinitis pigmentosa; pupillary light reflex; perimetry; chromatic pupilloperimetry

**Citation:** Sher I, Tucker Y, Gurevich M, Hamburg A, Bubis E, Kfir J, Zorani S, Derazne E, Skaat A, Rotenstreich Y. Chromatic pupilloperimetry measures correlate with visual acuity and visual field defects in retinitis pigmentosa patients. *Trans Vis Sci Tech.* 2020;9(8):10, <https://doi.org/10.1167/tvst.9.8.10>

**Purpose:** To evaluate the ability of chromatic pupilloperimetry to identify visual field (VF) defects in patients with retinitis pigmentosa (RP) and to test the correlation between pupilloperimetry impairment and retinal structural and functional measures.

**Methods:** The pupil responses of 10 patients with RP (mean age, 41.3 ± 16.2 years) and 32 healthy age-similar controls (mean age, 50.7 ± 15.5 years) for 54 focal blue and red stimuli presented in a 24-2 VF were recorded. The pupilloperimetry measures were correlated with Humphrey VF mean deviation, best-corrected visual acuity, and ellipsoid zone area.

**Results:** Substantially lower percentage of pupil contraction and maximal pupil contraction velocity (MCV) were recorded in patients with RP throughout the VF in response to blue and red stimuli. The mean absolute deviation (MADEV) in the latency of MCV (LMCV) was significantly larger in patients compared with controls for blue and red stimuli ( $P = 1.0 \times 10^{-7}$  and  $P = 1.0 \times 10^{-6}$ , respectively). The LMCV MADEV differentiated between patients and controls with high specificity and sensitivity (area under the receiver operating characteristic curve, 0.987 and 0.973 for blue and red, respectively). The MADEV of LMCV for blue stimuli correlated with best-corrected visual acuity ( $\rho = 0.938$ ,  $P = 5.9 \times 10^{-5}$ ) and ellipsoid zone area ( $\rho = -0.857$ ;  $P = 0.002$ ). The MADEV of LMCV for red stimuli correlated with Humphrey VF mean deviation ( $\rho = -0.709$ ;  $P = 0.022$ ). Minimizing the test to 15 targets maintained a diagnosis of retinal damage in patients with RP with high sensitivity and specificity (area under the receiver operating characteristic curve, 0.927).

**Conclusions:** The chromatic pupilloperimetry measures significantly correlated with retinal function and structure in patients with RP at various disease stages.

**Translational Relevance:** Chromatic pupilloperimetry may enable objective assessment of visual field defects and visual acuity in RP.

## Introduction

Retinitis pigmentosa (RP) is a group of incurable hereditary retinal degeneration diseases characterized by progressive degeneration of rod and cone photoreceptors. The worldwide prevalence of RP is 1 in 3500 to 4000.<sup>1</sup> The most common form of RP

is rod-cone dystrophy, in which the first symptom is night blindness, followed by a progressive peripheral visual field (VF) loss. Eventually, loss of function of macular cones results in a decrease in visual acuity and central vision loss. With the recent advances in gene therapy for RP, it is important to diagnose the disease early and to detect small and focal changes in retinal function.

The clinical standard for diagnosis and staging of RP and for evaluation of photoreceptor function is the electroretinogram (ERG).<sup>2,3</sup> A full-field ERG records the sum of potential from the whole retina; an abnormal full-field ERG will be recorded only if at least 20% of the photoreceptors have degenerated, and small focal changes in retinal function may not be detected. Multifocal ERG enables the assessment of ERG activity in small areas of retina and mapping of small scotomas.<sup>4</sup> However, the test is limited by the high test–retest variability in patients with RP, and patients with loss of central vision. Patients who are unable to maintain foveal fixation may not be able to perform the test.<sup>5</sup>

The use of perimetry is also recommended as part of the clinical evaluation of patients with RP to assess the extent of vision loss and for determination of legal blindness.<sup>3</sup> However, standard perimetry techniques are subjective and rely heavily on subjects' cooperation. In addition, once a moderate VF loss occurs, test–retest variability increases substantially, a reliable determination of VF change.<sup>5–7</sup>

Clinical structure and function studies suggest that photoreceptor loss in RP may be assessed by optical coherence tomography (OCT) and that VF parameters correlate with changes in OCT photoreceptor layer thickness.<sup>8–12</sup> Tee et al. demonstrated that the area of the photoreceptor inner segment/outer segment junction (ellipsoid zone [EZ]) measured in spectral domain OCT (SD-OCT) macular scans may be used as a structural biomarker to measure disease extent and progression in patients with RP.<sup>13</sup>

The afferent arm of the pupillary light reflex (PLR) is initiated by the photoreceptors, suggesting that the measurement of pupil response to light stimuli may reflect photoreceptor health. Pupillometry has several important advantages, including the objectivity of the test, the noninvasiveness of the procedure, and the minor cooperation needed from the patients.<sup>14</sup> Several clinical studies have successfully used chromatic pupillometry to assess the function of rods, cones, and ganglion cells in various diseases including RP.<sup>15–20</sup> However, because full-field light stimuli were used, with a stimulus size that was equal to or larger than 90°, the pupillometry measurements reflect the massed response from the whole retina and cannot be used to assess focal changes in photoreceptor function.

In previous studies, we demonstrated a proof of concept of using chromatic pupilloperimetry for the evaluation of focal rod and cone function in various retinal locations. Those studies indicated that cones significantly contribute to the pupil responses for focal red light stimuli, whereas pupil responses for focal blue light stimuli are mainly mediated by rods with

cone contributions.<sup>21–23</sup> Low test–retest variability was demonstrated and the pupil response of patients with RP measured by chromatic pupilloperimetry in a 16° VF correlated with dark adapted chromatic Goldmann perimetry.<sup>21,23</sup>

In the current study, we “mapped” the pupil response of control subjects and patients with RP for focal red and blue light under conditions that emphasized focal rod and cone activation. Light stimuli were presented in a spatial pattern similar to the 24-2 Humphrey perimetry test. We demonstrate a high correlation between the chromatic pupilloperimetry measures, subjective visual function (best-corrected visual acuity and Humphrey perimetry), and photoreceptor structure (EZ area [EZA]).

## Methods

The study was approved by The Sheba Medical Center Institutional Review Board Ethics Committee and was conducted according to the tenets of the Declaration of Helsinki. The trial was registered at [www.clinicaltrials.gov](http://www.clinicaltrials.gov) (NCT02014389). Informed written consent was obtained from all participants.

## Participants

The control group included 32 healthy volunteers (17 females and 15 males; ages 25–71 years old, mean age, 50 ± 14.7 years). Inclusion criteria were normal eye examination, best-corrected visual acuity of 20/20, normal color vision (Farnsworth/Lanthorn D-15 Test), no ocular disease, no use of any topical or systemic medications that could adversely influence efferent pupil movements, and a normal Humphrey 24-2 Swedish interactive threshold algorithm test (SITA standard protocol, Humphrey Field Analyzer II, Swedish interactive threshold algorithm 24-2; Carl Zeiss Meditec, Inc., Jena, Germany).

The patient group was comprised of 10 patients with RP (2 females and 8 males, ages 21–67 years, mean age, 41.3 ± 16.3 years). There was no significant difference in age (*t*-test  $P = 0.106$ ) and gender (Fisher's exact test  $P = 0.083$ ) between control and patient groups. Inclusion criteria were diagnosis of rod–cone degeneration RP (i.e., elevated final dark adaptation threshold of at least twice the normal value, retinal arteriolar narrowing, abnormal fundus appearance typical of RP, and previously recorded abnormal ERG under scotopic or photopic conditions or both) in compliance with the protocol of the International Society for Clinical Electrophysiology of Vision.<sup>24</sup> Exclusion criteria were

any atypical form of RP, patients with RP demonstrating a cystoid maculae edema on OCT, any other ocular disease such as glaucoma, uveitis, diabetic retinopathy, and posterior subcapsular cataract more than 11% of total lens area (i.e., equivalent to P3 on Lens Opacity Classification System III). Genetic testing was not required for study eligibility, but results of genetic testing were available for patient R7 (homozygous for the FAM161A c.1355\_6delCA null mutation).<sup>25</sup> The causative mutation in the other patients with RP has not been identified yet.

All participants underwent monocular visual acuity testing using a Snellen chart at a working distance of six meters under mesopic conditions in both eyes. Humphrey perimetry (HFA-II, Carl Zeiss, SITA Standard 24-2, stimulus size III), chromatic pupilloperimetry and SD-OCT testing were performed on the study eye. The study eye was selected randomly in all subjects. Thus, one-half of the subjects were tested on their right eye and one-half on their left eye.

### Chromatic Pupilloperimetry Testing

The chromatic pupilloperimetry testing was carried out under mesopic conditions ( $0.04 \text{ cd/m}^2$ ), after a 2-minute adaptation. The nontested eye was occluded. Participants were asked to fixate on a white light ( $6 \text{ cd/m}^2$ ) at the center of the device.<sup>22</sup> Small ( $0.43^\circ$ , Goldmann size III) red ( $624 \pm 5 \text{ nm}$ ,  $1000 \text{ cd/m}^2$ ) and blue ( $485 \pm 5 \text{ nm}$ ,  $170 \text{ cd/m}^2$ ) light stimuli were presented in a  $30^\circ$  VF from 54 light-emitting diodes using a chromatic pupilloperimeter (Accutome Inc., Malvern, PA). The location of the light-emitting diodes was selected to match the Humphrey Field Analyzer 24-2 test protocol that tests 54 points and measures  $24^\circ$  temporally and  $30^\circ$  nasally (Supplementary Fig. S1). Stimulus size was selected to align the stimulus protocol with standard automated perimetry. Light intensities were chosen based on previous studies in which presentation of small ( $0.43^\circ$ ) red light stimuli at intensity of  $1000 \text{ cd/m}^2$  and blue stimuli at  $170 \text{ cd/m}^2$  resulted in substantial maximal pupil contraction ( $\geq 10\%$ ) in peripheral and central VF locations in healthy subjects.<sup>21–23</sup> Those studies indicated that, under these test conditions, cones significantly contributed to the PLR for red light, and the PLR for blue light was mainly mediated by rods with cone contributions.<sup>21,22</sup> Light intensities were determined using LS-100 luminance meter (Konica Minolta, Tokyo, Japan). Stimulus duration was 1 second and the interstimulus interval was 4 seconds. These time intervals were chosen based on previous studies demonstrating the ability to measure the PLR for chromatic stimuli presented for 1 second, and the full recovery

of the pupil 3 seconds after light offset.<sup>21–23</sup> Pupil diameter was recorded by a computerized infrared high-resolution camera at a frequency of 30 Hz. The software (Accutome, Inc.) searched for the pupil in every image and reconstructed automatically the pupil response waveforms. Tests in which the subject blinked during the first 2.5 seconds after stimulus onset (contraction phase) were excluded automatically, and the targets were automatically retested.

### Pupil Response Parameters

A custom software was used to analyze the PLR parameters (Accutome Inc.).<sup>21–23</sup>

To compensate for tremor fluctuations in pupil size during fixation, standardized extreme optimization numerical libraries provided curve fitting functionality integrated into .NET architecture. By filtering pupil response data through both high-order polynomial and Savitzky-Golay filters included in these libraries, a smoothed waveform was achieved while maintaining key representation of input data. Five pupil response parameters were calculated and analyzed: the percentage of pupil contraction (PPC), the maximal contraction velocity (MCV in pixels per second), the latency of MCV (LMCV in seconds) as we previously described.<sup>21–23</sup> All pupil response parameters were determined based on the smoothed waveforms.

The PPC values were normalized for each test target based on the initial pupil size measured at the beginning of each stimulus, using the formula:

$$PPC = \frac{\text{Initial pupil diameter} - \text{Minimum pupil diameter}}{\text{Initial pupil diameter}} \quad (1)$$

If recording of the pupil response failed more than four times at a certain VF test location, the data of that test point was not included in the analysis. The mean absolute deviation (MADEV) in LMCV recordings between various test points was measured as previously described.<sup>21,23</sup> Briefly, the mean value of LMCV recorded at 54 locations and the absolute differences between the mean LMCV and the LMCV values recorded at each location were determined. The mean of all absolute differences was calculated to give the LMCV MADEV for each subject.

This is expressed by the following equations:  $LMCV \text{ MADEV} = \frac{\sum_{i=1}^N |L_i - \bar{L}|}{N}$ , where  $i = 1 \dots N$  denotes test target index ( $N = 54$ ),  $L_i$  is the LMCV recorded in test target ( $i$ ), and  $\bar{L}$  is the mean LMCV recorded for that individual across the VF.

## SD-OCT EZA

Macular scans were performed with Heidelberg Spectralis SD-OCT (Heidelberg Engineering, Heidelberg, Germany). Horizontal high-resolution transfoveal line scans were obtained using automated real-time tracking with an average of nine images. Each volume scan was composed of 25 horizontal b-scans in high-resolution mode with 256  $\mu\text{m}$  distance between b-scans and 512 a-scans per b-scan. The EZA was measured using vendor software (Heidelberg Eye Explorer Version 1.10.2.0). The observers marked the locations of the two most distant temporal and nasal points that the EZ layer could be distinguished from the adjacent layers using the “arrow tool” at each scan (Supplementary Fig. S2b). The dots were connected to generate a circle using the “draw region” tool of the software, and the circle’s area was automatically calculated by software (Supplementary Fig. S2a). The EZA was measured by three observers (YT, AH, JK) and the mean of the three measurements was used for analysis.

## Statistical Analysis

Age and gender of the study groups were compared using the Student *t*-test and Fisher’s exact test, respectively. Test points in which the device failed to record the pupil response were not included in the statistical analysis. Left eye pupilloperimetry data were mirrored to a right eye format for statistical analysis.

The pupilloperimetry maps were divided into seven corresponding sectors according to the Garway-Heath scheme.<sup>26</sup> The area under the receiver operating characteristic curve (ROC AUC) was calculated in each sector using the predicted value of mean of response obtained from generalized estimating equation logistic model with repeated measures (measures from the same subject in each GH sector from various VF test targets, Supplementary Fig. S10). Generalized estimating equation models included intercept, distribution = binomial, link = logit, criteria method = Fisher, scale = 1, maximum iterations = 100, convergence criteria included change in parameter estimates minimum  $1\text{E-}6$  type absolute, singularity tolerance  $1\text{E-}12$ , model effects = analysis type III. Models were constructed for PPC and MCV in response for blue and red light stimulus, and adjusted for subject age.

Mann–Whitney test was used to determine the difference in the MADEV between groups. The robustness of using the LMCV MADEV for discrimination between control and RP groups was examined by calculating ROC AUC. Spearman correlation was used to assess the association between the patients’ LMCV MADEV and their Humphrey VF mean devia-

tion (HVF-MD) score and EZA. All statistical analyses were performed using the SPSS Statistics for Windows, Version 23.0 (IBM Corporation, Armonk, NY).

## Results

### Characterization of Pupil Responses to Focal Chromatic Light Stimuli in Control Participants

We initially characterized the pupil response to focal chromatic light stimuli presented at a pattern similar to HVF 24-2 in control participants. Color-coded maps of the mean PPC, MCV, and LMCV recorded in each test target in response to blue and red light stimuli in the control group are presented in Supplementary Figs. S3 to S5. The mean PPC ranged from  $10\% \pm 6\%$  to  $17\% \pm 6\%$  in response to blue light (Supplementary Fig. S3A). Lower values were recorded in response to red light ( $4\% \pm 3\%$  to  $12\% \pm 6\%$ ; Supplementary Fig. S3B), even though the red-light stimuli were presented at a five-fold higher intensity than the blue light stimuli. Higher mean PPC values were recorded in response to red light stimuli presented at central ( $10\%–12\%$ ; standard deviation,  $5\%–7\%$ ) and temporal ( $8\%–9\%$ ; standard deviation,  $4\%–5\%$ ) compared with nasal ( $5\%–6\%$ ; standard deviation,  $4\%–5\%$ ) VF test targets. A similar spatial pattern was observed in the MCV measurements. Thus, higher mean MCV values were recorded throughout the VF in response to blue light stimuli compared with red light stimuli (ranging between 17 and 27 pixel/s [standard deviation, 9–10 pixel/s] vs. 8–19 pixel/s, [standard deviation, 5–9 pixel/s], respectively) and higher mean MCV values were recorded in response to red light stimuli presented at central (16–19 pixel/s, standard deviation, 8–9 pixel/s) and temporal (15–17 pixel/s, standard deviation, 8–10 pixel/s) compared with nasal (8–11 pixel/s, standard deviation, 5–7 pixel/s) VF test targets (Supplementary Fig. S4A and B). The mean LMCV recordings ranged from  $0.71 \pm 0.24$  seconds to  $0.78 \pm 0.29$  seconds and  $0.70 \pm 0.14$  seconds to  $0.86 \pm 0.4$  seconds in response to blue and red light, respectively (Supplementary Fig. S5A and B).

### Patients With RP Present Substantially Lower PPC and MCV Throughout the 24-2 VF

Patients with RP were divided into two groups according to the extent of VF loss as determined by Humphrey perimetry. Group A included three patients who had partial VF loss, and group B

consisted of seven patients with total VF loss (Table 1). Figure 1 demonstrates color-coded maps of the mean PPC recorded in each test point location in response to blue and red light stimuli in the three study groups. The color in each location represents the calculated standard error (SE) from the mean of the control group in that location. The mean PPC recorded in RP group A ranged from  $1\% \pm 1\%$  to  $16\% \pm 13\%$  in response to blue light and from  $1\% \pm 1\%$  to  $15\% \pm 15\%$  in response to red light. In RP group B, the mean PPC values ranged from  $1\% \pm 1\%$  to  $10\% \pm 6\%$  in response to blue light and from  $1\% \pm 0.4\%$  to  $13\% \pm 6\%$  in response to red light. Maps of the standard deviation for patients' PPC are presented in Supplementary Figures S6 and S7.

The mean PPC for blue light was lower by more than 2 SEs from the mean of controls in 94% and 100% of the test targets in RP groups A and B, respectively (Figs. 1C, E). By contrast, the mean PPC for red light was lower by more than 2 SEs from the mean of controls only in 63% and 61% of the test targets in groups A and B, respectively (Figs. 1, D, F).

The mean MCV for blue light was lower by over 2 SEs from the mean of controls in 89% and in 100% of the test targets in RP groups A and B, respectively (Figs. 2C, D). The mean MCV for red light was lower by more than 2 SEs from the mean of controls in 85% and 93% of the test targets in RP groups A and B, respectively (Figs. 2E, F).

### The LMCV MADEV Is Higher in Patients With RP and Correlates With Patients' Visual Function and Photoreceptor Loss

Unlike the control group, in which the mean LMCV values were similar across VF locations (ranging from  $0.70 \pm 0.23$  seconds to  $0.86 \pm 0.4$  seconds; Supplementary Figs. S5A, B and Figs. 3A, B), the RP group presented high variability in LMCV recorded at various VF locations. The mean LMCV values ranged from  $0.60 \pm 0.35$  seconds to  $1.19 \pm 0.20$  seconds in response to blue light and from  $0.60 \pm 0.24$  seconds to  $1.42 \pm 0.60$  seconds in response to red light in RP group A (Figs. 3C, D). In RP group B, the mean LMCV ranged from  $0.40 \pm 0.20$  seconds to  $1.42 \pm 0.41$  seconds and from  $0.45 \pm 0.30$  seconds to  $1.48 \pm 0.47$  seconds in response to blue and red light stimuli, respectively (Figs. 3E, F). The interquartile range of the LMCV recorded in patients with RP was substantially larger than the interquartile range of the LMCV recorded in controls for both colors (Supplementary Figs. S8 and S9).

To evaluate the extent of variability in LMCV between VF locations, we determined for each subject the MADEV. The mean value of LMCV recorded at

54 locations across the entire VF was determined for each subject. Then, the absolute differences between the mean LMCV and the LMCV values recorded at each location were determined. The mean of all absolute differences was calculated to give the MADEV for each subject. The LMCV MADEV for blue light was significantly smaller in control subjects compared with patients with RP (mean,  $0.036 \pm 0.027$  seconds vs. mean,  $0.35 \pm 0.17$  seconds;  $P = 1.0 \times 10^{-7}$ ; Supplementary Table). The LMCV MADEV for red light was also significantly smaller in control subjects compared with patients with RP (mean,  $0.093 \pm 0.067$  seconds vs. mean,  $0.41 \pm 0.13$  seconds;  $P = 1.0 \times 10^{-6}$ ; Supplementary Table). A ROC analysis demonstrated that LMCV MADEV differentiated between patients and controls with high specificity and sensitivity (AUC = 0.987 and 0.973 for blue and red light, respectively).

The LMCV MADEV for the red light in patients with RP correlated with their BCVA (Spearman's rho = 0.677;  $P = 0.003$ ; Fig. 4A) and HVF-MD (Spearman's rho =  $-0.709$ ;  $P = 0.022$ , Fig. 4B). A lower correlation was observed between this parameter and the EZA (Spearman's rho =  $-0.607$ ;  $P = 0.063$ , Fig. 4C).

A strong and significant correlation was obtained between the patients' LMCV MADEV in response to blue light and their BCVA (Spearman's rho = 0.938;  $P = 5.9 \times 10^{-5}$ ; Fig. 5A) and SD-OCT EZA (Spearman's rho =  $-0.857$ ;  $P = 0.002$ ; Fig. 5C). A lower association was observed with the HVF-MD (Spearman's rho =  $-0.503$ ;  $P = 0.138$ ; Fig. 5B).

As an example, RP group A patients R5 and R8 had the smallest LMCV MADEV for both red and blue light (Supplementary Table and Supplementary Figs. S8 and S9). These patients had good BCVA (0 and 0.1 log MAR, respectively), relatively small negative HVF-MD ( $-11.59$  dB and  $-14.4$  dB, respectively), and the largest EZA out of all the patients with RP ( $6.85$  mm<sup>2</sup> and  $7.19$  mm<sup>2</sup>, respectively, Table 1). Interestingly, RP group B patient R9 had a small LMCV MADEV for blue light (0.108 seconds) and a measurable EZA (2.05 mm<sup>2</sup>) as well as normal BCVA. However, this patient presented with a large LMCV MADEV for red light (0.433 seconds) and nearly complete loss of Humphrey VF (MD =  $-31.59$  dB). ERG testing of this patient demonstrated that the photopic single flash was more affected than the scotopic ERG response, suggesting that the cones of this patient are more affected than the rods compared with the other patients (Table 1).

### Clustering Analysis

Next, we examined whether fewer test point locations could be used for RP diagnosis to decrease



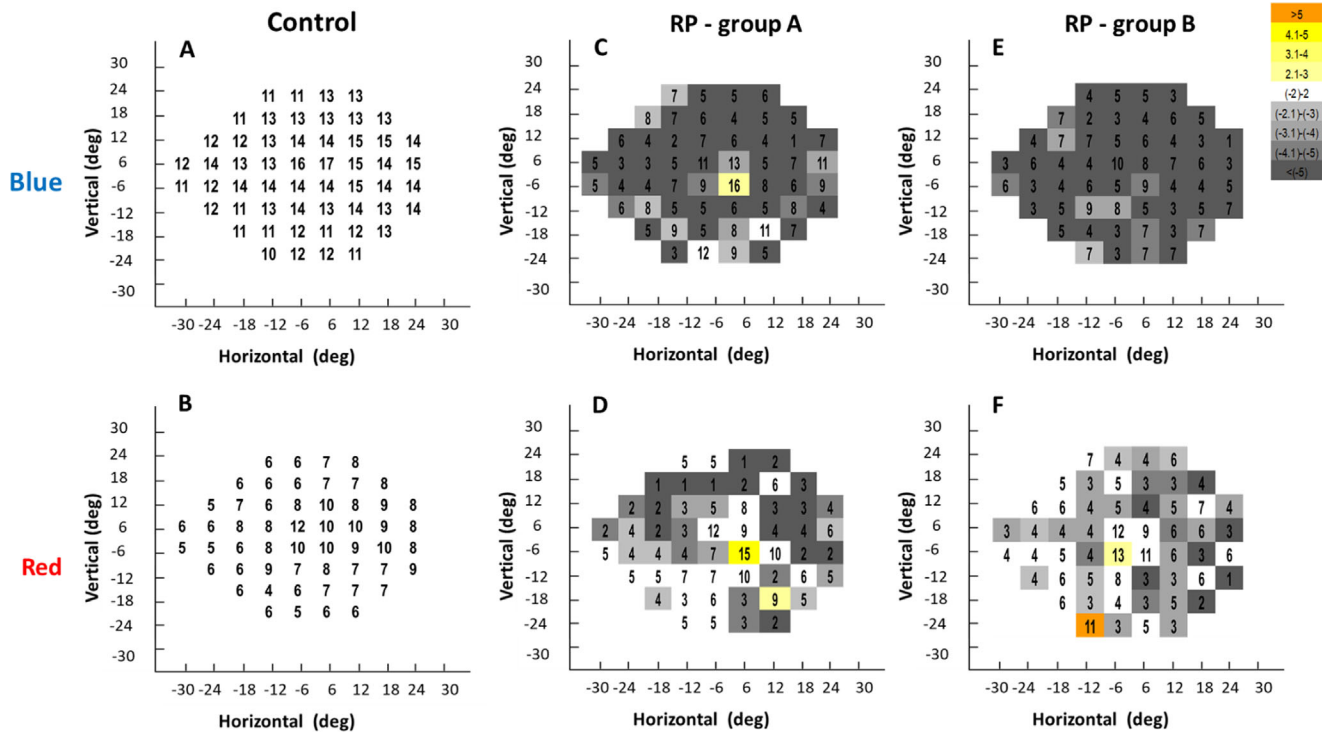


**Figure 1.** The PPC recorded in response to focal red and blue light stimuli at 54 VF test points in control and RP groups. The mean PPC recorded in response to blue (A, C, E) and red (B, D, F) focal light stimuli presented at 54 VF test points in control (A, B), RP group A (C, D), and RP group B (E, F) patients. Color coding is based on the number of SEs from the mean of controls and is shown on the right. *White* indicates that the mean value recorded in the patients equals to or is lower than two SEs from the mean of controls and *dark gray* indicates that the mean value recorded in the patients is lower by more than five SEs from the mean of controls.

testing time. To this aim, the pupilloperimetry parameters PPC and MCV recorded in each test target were clustered into seven sectors following the Garway-Heath scheme that divided the VF into sectors based on the corresponding optic nerve head regions (Supplementary Fig. S10).<sup>26</sup> The ROC AUC was calculated for PPC and MCV in each sector, as detailed in the Methods section. As shown in Table 2, higher AUC values were obtained for the pupilloperimetry parameters recorded in response to blue light than red light. MCV recorded in response to blue light had an AUC of more than 0.9 in four sectors, located in the superior (sectors 5 and 6, Supplementary Fig. S10) and temporal (sectors 1 and 7) VF. The highest AUC were recorded in sectors 5 and 7 (AUC = 0.927 and AUC = 0.941, respectively).

### Individual Cases

#### RP Group A: Patient R8

The pupilloperimetry results of RP group A patient R8 are presented in Figure 6. A qualitative agreement was observed between the patient’s Humphrey VF and

the chromatic pupilloperimetry maps. PPC and MCV values lower than 2 SEs from the mean of controls (marked with gray color; Figs. 6B–E) were recorded in areas with diminished light sensitivity by Humphrey VF (Fig. 6A). The inferior and central VF were more preserved by the Humphrey perimetry. PPC and MCV within 2 SEs from the mean of controls (white color) or higher than the mean of controls (yellow-orange color) were recorded in these VF areas in response to red light (Figs. 6D, E). By contrast, the PPC recorded in response to blue light in these areas was lower by more than 2SEs from the mean of controls, suggesting a possible defect in rod function (Fig. 6B). The patient had a small LMCV MADEV for both red and blue light (0.145 seconds and 0.142 seconds, respectively), a HVF-MD score of  $-14.44\text{dB}$ , and the largest EZA out of all patients with RP ( $7.19\text{ mm}^2$ ).

#### RP Group B: Patient R7

Patient R7 was homozygous for the FAM161A c.1355\_6delCA null mutation. He presented with undetectable ERG responses and a complete loss of VF by Humphrey perimetry (Fig. 7A). The chromatic

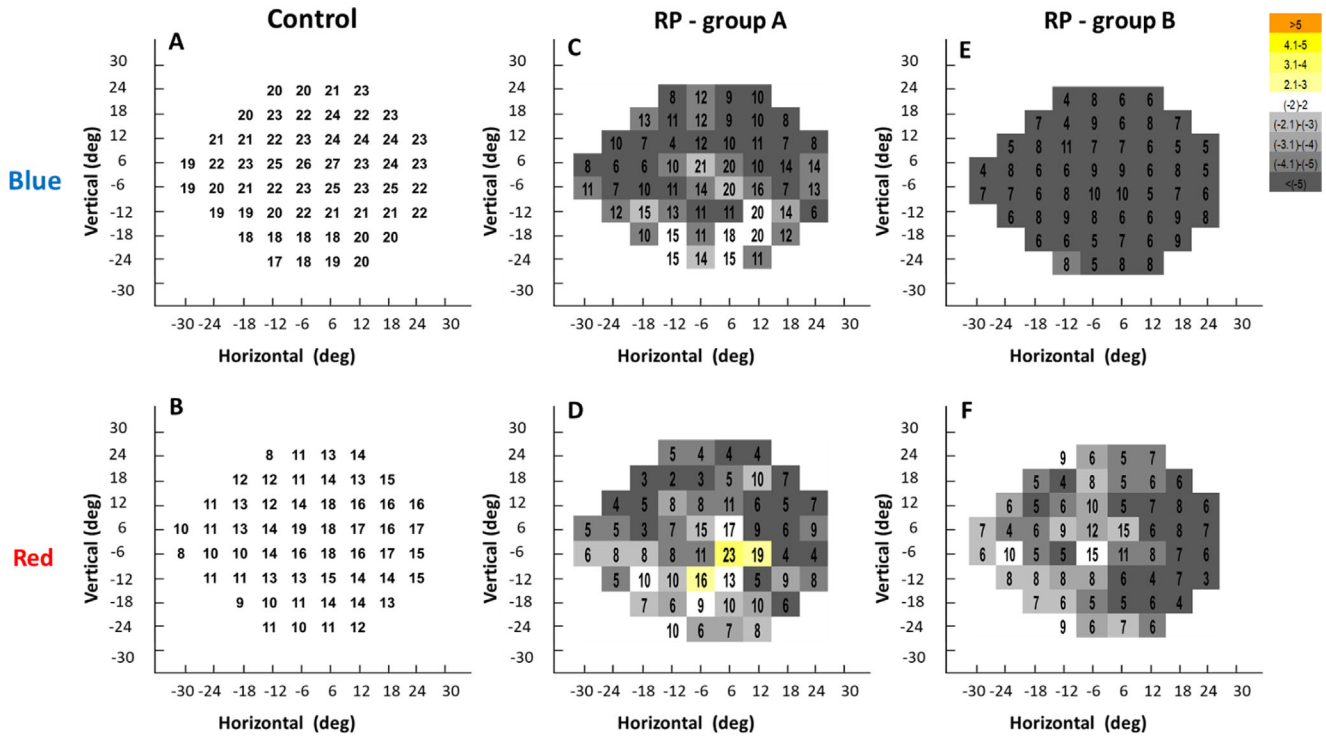


**Figure 2.** MCV recorded in response to focal red and blue light stimuli at 54 VF test points in control and RP groups. The mean MCV (in pixels per second) recorded in response to blue (A, C, E) and red (B, D, F) light stimuli presented at 54 VF test points in control (A, B), RP group A (C, D), and RP group B (E, F) patients. Color coding is as described in Figure 1.

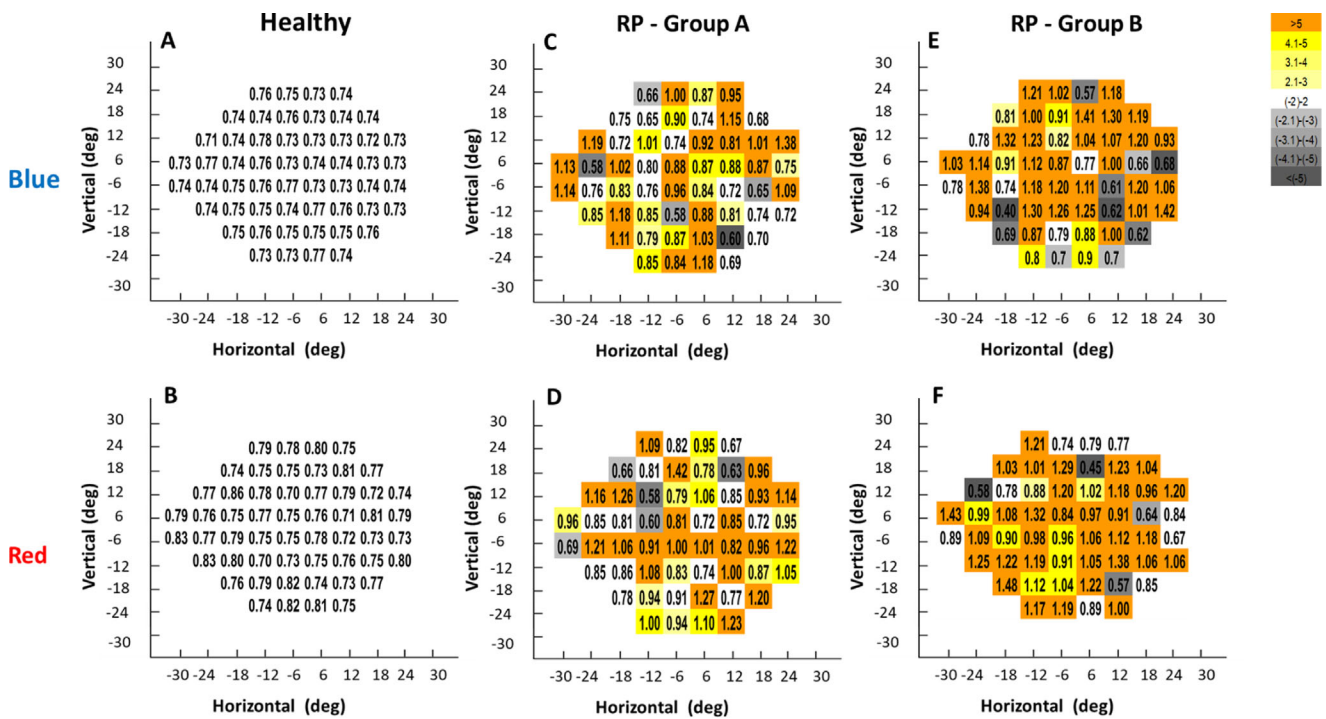


**Figure 3.** LMCV recorded in response to focal red and blue light stimuli at 54 VF test points. The mean LMCV (in seconds) recorded in response to blue (A, C, E) and red (B, D, F) light stimuli presented at 54 VF test points in control (A, B), RP group A (C, D) and RP group B (E, F) patients. Color coding is as described in Figure 1.



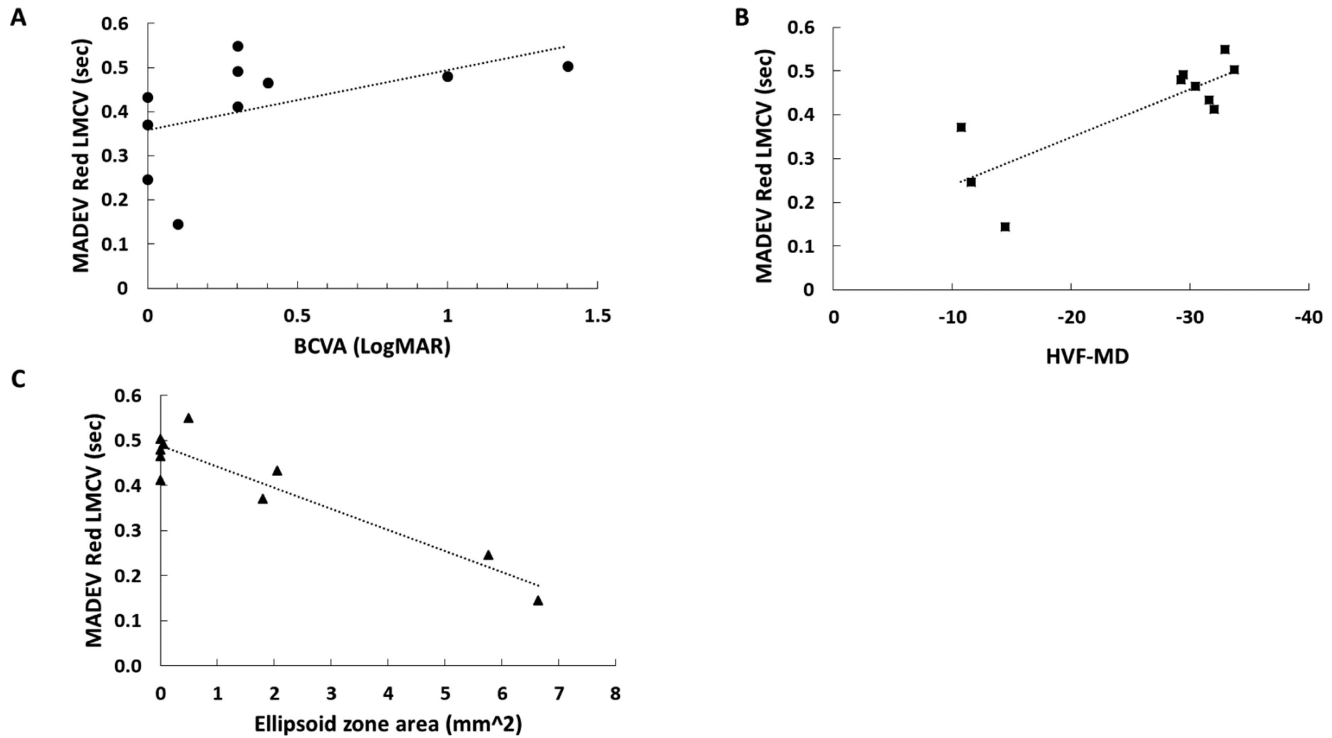


**Figure 4.** Linear correlation between the MADEV in the LMCV recorded in patients with RP in response to focal red light stimuli, visual function, and retinal structure. Linear correlation between the LMCV MADEV recorded in patients with RP in response to focal red light stimuli (y-axis in all graphs) and best-corrected visual acuity (BCVA, A), HVF-MD score (B) and the EZA measured by SD-OCT (C). LogMAR, logarithm of the minimum angle of resolution.

pupilloperimetry maps of this patient demonstrated a substantial defect in pupil response throughout the VF, with PPC and MCV values lower than 5 SEs from the mean of controls in nearly all VF locations (marked by a dark gray color in Figs. 7B–E). However, in the vast majority of retinal locations, the PPC and MCV were recordable in response to both red and blue light stimuli, suggesting that the chromatic pupilloperimetry may enable the assessment of remaining function of photoreceptors at various retinal locations that are below the detection levels of Humphrey perimetry and ERG. The LMCV MADEV recorded for both red and blue light was large (0.55 seconds and 0.43 seconds, respectively), correlating with a large negative Humphrey perimetry MD (−32.90 dB) and a small EZA by SD-OCT (0.67 mm<sup>2</sup>).

patients with RP at various disease stages, demonstrating the potential of using this method for the objective assessment of visual function in RP.

The chromatic pupilloperimetry global score of LMCV MADEV recorded in response to blue light stimuli differentiated between controls and patients with RP with a ROC AUC of 0.987 and significantly correlated with BCVA and the area of the photoreceptor inner segment EZ by SD-OCT. These data suggest that this pupilloperimetry parameter may potentially be useful as an objective noninvasive measure for defects in retinal function and visual acuity. The good correlation with the EZA suggests that chromatic pupilloperimetry could provide insight into photoreceptor loss in RP. Our findings are in agreement with the study of Tee et al.,<sup>13</sup> which demonstrated a significant correlation between BCVA and EZA in patients with RP.

A qualitative correlation was found between the PPC and MCV measured in response for focal red light stimuli and the Humphrey 24-2 total deviation results. In addition, a good correlation was observed between the LMCV MADEV for red light and the HVF-MD score, suggesting that focal pupil

## Discussion

The results of this study show that the chromatic pupilloperimetry measures correlate with visual acuity, Humphrey VF, and photoreceptor degeneration in

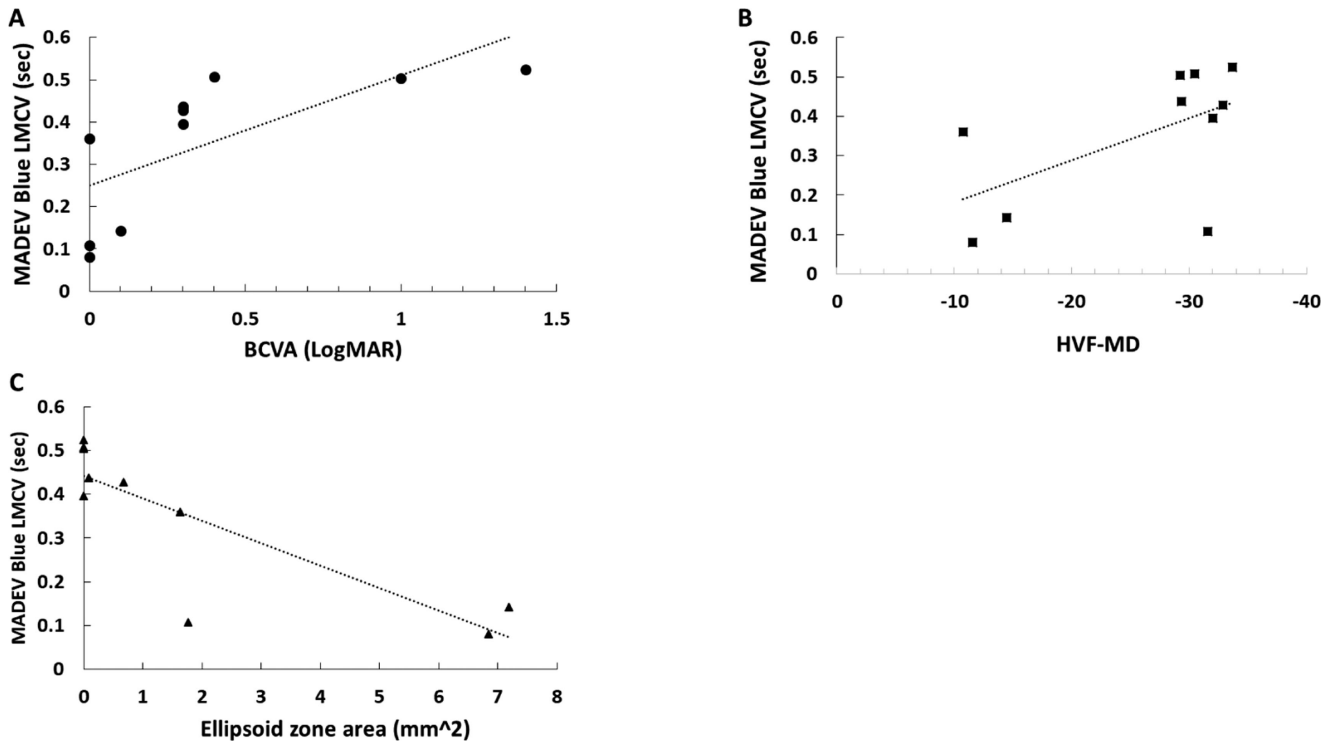


**Figure 5.** Linear correlation between the LMCV MADEV recorded in patients with RP in response to focal blue light stimuli, visual function, and retinal structure. Linear correlation between the LMCV MADEV recorded in patients with RP in response to focal blue light stimuli (y-axis in all graphs) and best corrected visual acuity (BCVA, A), HVF-MD score (B) and the EZA measured by SD-OCT (C). LogMAR, logarithm of the minimum angle of resolution.

response to red light may potentially be used for objective assessment of VF at various stages of RP. These results are in agreement with the fact that the Humphrey perimetry test was performed using the SITA standard protocol that includes a background lighting of 31.5 abs and measures mainly the function of cones,<sup>27</sup> as well as with a previous study with healthy subjects that demonstrated that the cones considerably contribute to the pupil response for focal red light stimuli presented at central and peripheral retinal locations.<sup>22</sup> Our hypothesis that the cones contribute considerably to the pupil response for focal red light throughout the 24-2 VF is further supported by the data demonstrating that larger mean PPC and MCV were recorded in the control group in response to focal red light stimuli presented at the central and temporal VF locations compared with nasal VF targets, correlating with a higher cone-rod ratio at the macula and nasal retina compared with temporal retina.<sup>28</sup>

Our data that the mean PPC for blue light in control subjects was larger than the mean PPC for red light across the VF even though the blue light was presented at a six-fold lower intensity than the

**Table 2.** The ROC AUC Obtained for Each Chromatic Pupilloperimetry Parameter at the Seven VF Sectors

Sector	Blue		Red	
	PPC	MCV	PPC	MCV
1	0.855	0.924	0.815	0.890
2	0.805	0.845	0.680	0.772
3	0.843	0.878	0.696	0.762
4	0.820	0.884	0.679	0.748
5	0.882	0.927	0.734	0.814
6	0.861	0.919	0.739	0.813
7	0.878	0.941	0.824	0.886

The ROC AUC was calculated for PPC and MCV in each sector (see Supplementary Fig. S10) using the predicted value of mean of response obtained from generalized estimating equation logistic model with repeated measures (measures from the same subject in each sector from various VF test targets). The models were constructed for blue and red light stimuli and were adjusted for patient age.

red light, suggest that rods have a substantial contribution to the pupil response for blue light. These

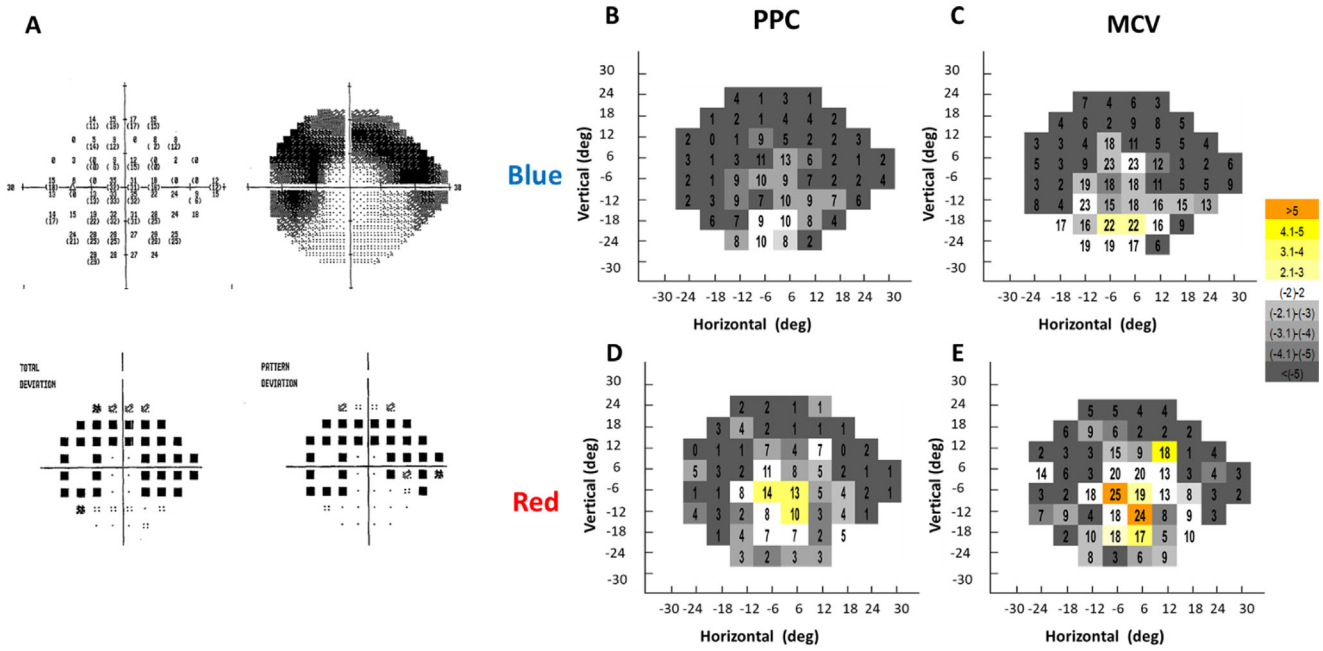


**Figure 6.** Chromatic pupilloperimetry results of patient R8. (A) Humphrey 24-2 perimetry testing results. (B, D) The PPC recorded in response to blue (B) and red (D) focal light stimuli presented at 54 VF test points. (C, E) The MCV (in pixels per second) recorded in response to blue (C) and red (E) focal light stimuli presented at 54 VF test points. Color coding is as described in Figure 1.

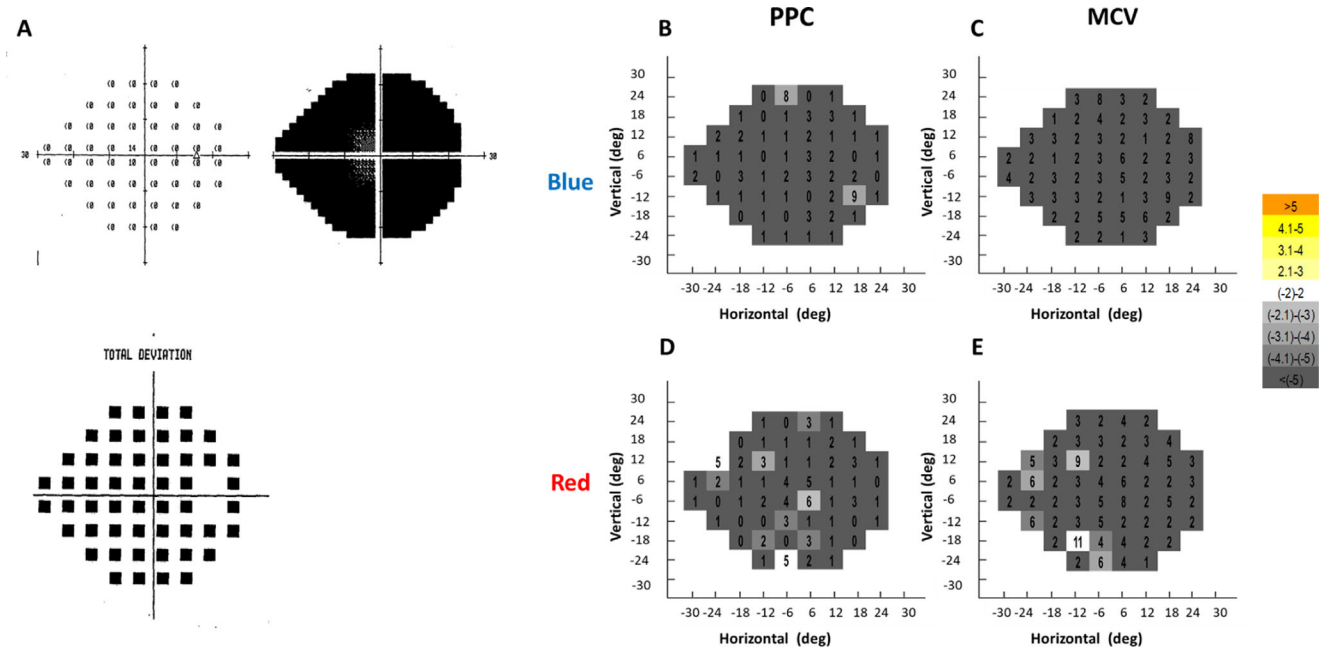


**Figure 7.** Chromatic pupilloperimetry results of patient R7. (A) Humphrey 24-2 perimetry testing results. (B, D) The PPC recorded in response to blue (B) and red (D) focal light stimuli presented at 54 VF test points. (C, E) The MCV (in pixels per second) recorded in response to blue (C) and red (E) focal light stimuli presented at 54 VF test points. Color coding is as described in Figure 1.

findings are in agreement with previous studies indicating that the PLR for focal small blue light stimuli presented at low light intensities are mainly mediated by rods.<sup>22</sup> The findings that control subjects presented with higher mean PPC values in response to blue

light stimuli in central VF test targets compared with peripheral VF test targets suggest that cones also contribute to the response to blue light with a greater contribution of cones in the center of the VF. In patients with RP, the cone contribution to the PLR

for blue light is most likely larger than in controls, as reflected by the similar pattern and PPC ranges of blue and red responses in the patients. The lower pupil response for red and blue light recorded in the patients is in agreement with studies using full-field blue and red light stimuli that demonstrated decreased rod- and cone-mediated pupil responses in patients with RP.<sup>16,29</sup>

The clustering analysis suggested that it may be possible to use fewer test targets for diagnosis of retinal damage in patients with RP while maintaining high specificity and sensitivity using the MCV measure in response for blue light. ROC AUC of greater than 0.9 were recorded for this chromatic pupilloperimetry measure in the superior-temporal VF sectors (sectors 1, 5, 6, and 7; [Table 2](#) and Supplementary Fig. S10), in agreement with the typical superior-temporal VF loss in patients with RP.<sup>30</sup> The highest sensitivity and specificity were obtained in this clustering analysis in sector 7, which is composed of 2 test targets, and sector 5, which is composed of 13 test points. Pupilloperimetry recording in response to blue light in 15 test points is predicted to take less than 2 minutes, which significantly decreases the testing time.

Larger responses than the mean of controls were recorded in some patients with RP in areas with persevered sensitivity by Humphry perimetry. These large responses may represent hypersensitivity of the retinal cells or ganglion cells as part of the degeneration process. Hyperactivation of retinal ganglion cells was recently demonstrated in the retina of rodents undergoing photoreceptor degeneration.<sup>31,32</sup> Future studies with a larger cohort of patients with RP at various disease stages may shed more light on these findings.

Our study is limited by the small number of patients and the single visit testing. Future studies will include a larger number of patients and a trial duration of several years to determine the rate of progression of the chromatic pupilloperimetry measures. The longitudinal study will enable to assess the feasibility of using this method for disease progression monitoring. Nevertheless, the patients with RP who participated in this study were at different severity levels of the disease. Some of the patients had a recordable dark-adapted ERG, normal BCVA, and a measurable EZA (group A), whereas others had no recordable ERG or EZA and a deteriorated BCVA (patients in group B). In all patients with RP, the pupil responses were measurable at vast majority of the VF locations, suggesting that chromatic pupilloperimetry may enable objective and sensitive measurement of the remaining cone and rod function, even in a severely degenerated retina.

## Acknowledgments

Supported by Accutome, Inc., PA, USA. Accutome Inc. personnel participated in review of the article, but had no role in the design or conduct of this research.

Disclosure: **I. Sher**, Sheba Medical Center (P); **Y. Tucker**, None; **M. Gurevich**, None; **A. Hamburg**, None; **E. Bubis**, None; **J. Kfir**, None; **S. Zorani**, None; **E. Derazne**, None; **A. Skaat**, None; **Y. Rotenstreich**, Sheba Medical Center (P)

## References

- Hartong DT, Berson EL, Dryja TP. Retinitis pigmentosa. *Lancet*. 2006;368:1795–1809.
- Fishman GA, Birch DG, Holder GE, Brigell MG. Electrophysiologic testing in disorders of the retina, optic nerve, and visual pathway. San Francisco: The Foundation of the American Academy of Ophthalmology; 2001.
- Recommendations on clinical assessment of patients with inherited retinal degenerations-2016. *American Academy of Ophthalmology Clinical Education/Guidelines/Clinical Statements*. 2016; Accessed January 15, 2020
- Sutter E. Noninvasive testing methods: multifocal electrophysiology. 2010;10:1016.
- Seiple W, Clemens CJ, Greenstein VC, Carr RE, Holopigian K. Test-retest reliability of the multifocal electroretinogram and Humphrey visual fields in patients with retinitis pigmentosa. *Doc Ophthalmol*. 2004;109:255–272.
- Kim LS, McAnany JJ, Alexander KR, Fishman GA. Intersession repeatability of Humphrey perimetry measurements in patients with retinitis pigmentosa. *Invest Ophthalmol Vis Sci*. 2007;48:4720–4724.
- Bittner AK, Ibrahim MA, Haythornthwaite JA, Diener-West M, Dagnelie G. Vision test variability in retinitis pigmentosa and psychosocial factors. *Optom Vis Sci*. 2011;88:1496–1506.
- Hood DC, Lin CE, Lazow MA, Locke KG, Zhang X, Birch DG. Thickness of receptor and post-receptor retinal layers in patients with retinitis pigmentosa measured with frequency-domain optical coherence tomography. *Invest Ophthalmol Vis Sci*. 2009;50:2328–2336.
- Birch DG, Wen Y, Locke K, Hood DC. Rod sensitivity, cone sensitivity, and photoreceptor layer thickness in retinal degenerative diseases. *Invest Ophthalmol Vis Sci*. 2011;52:7141–7147.

10. Hood DC, Ramachandran R, Holopigian K, Lazow M, Birch DG, Greenstein VC. Method for deriving visual field boundaries from OCT scans of patients with retinitis pigmentosa. *Biomedical Optics Express*. 2011;2:1106–1114.
11. Lazow MA, Hood DC, Ramachandran R, et al. Transition zones between healthy and diseased retina in choroideremia (CHM) and Stargardt disease (STGD) as compared to retinitis pigmentosa (RP). *Invest Ophthalmol Vis Sci*. 2011;52:9581–9590.
12. Birch DG, Locke KG, Wen Y, Locke KI, Hoffman DR, Hood DC. Spectral-domain optical coherence tomography measures of outer segment layer progression in patients with X-linked retinitis pigmentosa. *JAMA Ophthalmol*. 2013;131:1143–1150.
13. Tee JJJ, Yang Y, Kalitzeos A, Webster A, Bainbridge J, Michaelides M. Natural history study of retinal structure, progression and symmetry using ellipsoid zone metrics in RPGR-associated retinopathy. *Am J Ophthalmol*. 2018; 198:111–123.
14. Kelbsch C, Strasser T, Chen Y, et al. Standards in pupillography. *Front Neurol*. 2019;10:129.
15. Kardon R, Anderson SC, Damarjian TG, Grace EM, Stone E, Kawasaki A. Chromatic pupil responses: preferential activation of the melanopsin-mediated versus outer photoreceptor-mediated pupil light reflex. *Ophthalmology*. 2009;116:1564–1573.
16. Kardon R, Anderson SC, Damarjian TG, Grace EM, Stone E, Kawasaki A. Chromatic pupillometry in patients with retinitis pigmentosa. *Ophthalmology*. 2011;118:376–381.
17. Kawasaki A, Munier FL, Leon L, Kardon RH. Pupillometric quantification of residual rod and cone activity in Leber congenital amaurosis. *Arch Ophthalmol*. 2012;130:798–800.
18. Kawasaki A, Crippa SV, Kardon R, Leon L, Hamel C. Characterization of pupil responses to blue and red light stimuli in autosomal dominant retinitis pigmentosa due to NR2E3 mutation. *Invest Ophthalmol Vis Sci*. 2012;53:5562–5569.
19. Lorenz B, Strohmayer E, Zahn S, et al. Chromatic pupillometry dissects function of the three different light-sensitive retinal cell populations in RPE65 deficiency. *Invest Ophthalmol Vis Sci*. 2012;53:5641–5652.
20. Kelbsch C, Maeda F, Lisowska J, et al. Analysis of retinal function using chromatic pupillography in retinitis pigmentosa and the relationship to electrically evoked phosphene thresholds. *Acta Ophthalmol*. 2017;95:e261–e269.
21. Chibel R, Sher I, Ner DB, et al. Chromatic multifocal pupillometer for objective perimetry and diagnosis of patients with retinitis pigmentosa. *Ophthalmology*. 2016;123:1898–1911.
22. Haj Yahia S, Hamburg A, Sher I, et al. Effect of stimulus intensity and visual field location on rod- and cone-mediated pupil response to focal light stimuli. *Invest Ophthalmol Vis Sci*. 2018;59:6027–6035.
23. Ben Ner D, Sher I, Hamburg A, et al. Chromatic pupilloperimetry for objective diagnosis of Best vitelliform macular dystrophy. *Clin Ophthalmol*. 2019;13:465.
24. McCulloch DL, Marmor MF, Brigell MG, et al. ISCEV Standard for full-field clinical electroretinography (2015 update). *Doc Ophthalmol*. 2015;130:1–12.
25. Bandah-Rozenfeld D, Mizrahi-Meissonnier L, Farhy C, et al. Homozygosity mapping reveals null mutations in FAM161A as a cause of autosomal-recessive retinitis pigmentosa. *Am J Human Genet*. 2010;87:382–391.
26. Garway-Heath DF, Poinosawmy D, Fitzke FW, Hitchings RA. Mapping the visual field to the optic disc in normal tension glaucoma eyes. *Ophthalmology*. 2000;107:1809–1815.
27. Johnson C, Keltner JL, Balestrery F. Static and acuity profile perimetry at various adaptation levels. *Doc Ophthalmol*. 1981;50:371–388.
28. Curcio CA, Sloan KR, Kalina RE, Hendrickson AE. Human photoreceptor topography. *J Comp Neurol*. 1990;292:497–523.
29. Park JC, Moura AL, Raza AS, Rhee DW, Kardon RH, Hood DC. Toward a clinical protocol for assessing rod, cone, and melanopsin contributions to the human pupil response. *Invest Ophthalmol Vis Sci*. 2011;52:6624–6635.
30. Grover S, Fishman GA, Brown J, Jr. Patterns of visual field progression in patients with retinitis pigmentosa. *Ophthalmology*. 1998;105:1069–1075.
31. Telias M, Denlinger B, Helft Z, Thornton C, Beckwith-Cohen B, Kramer RH. Retinoic acid induces hyperactivity, and blocking its receptor unmasks light responses and augments vision in retinal degeneration. *Neuron*. 2019;102:574–586. e5.
32. Denlinger B, Helft Z, Telias M, Lorach H, Palanker D, Kramer RH. Local photoreceptor degeneration causes local pathophysiological remodeling of retinal neurons. *JCI Insight*. 2020;5:e132114.